Progress In Electromagnetics Research C, Vol. 133, 109–120, 2023

A Novel Quadrangular Slotted DGS with a Wideband Monopole Radiator for Fifth-Generation Sub-6 GHz Mid-Band Applications

Idrish Shaik[1, *] and Krishna V. Sahukara[2]

Abstract—The demand for high data rate, good channel capacity, and reliability is always the primary area of concern in the modern era of wireless communication systems. The 5G standards have the fortitude to bring about rapid data transfer speeds, instantaneous connectivity, large data capacities, and minimal latency. In this paper, a novel quadrangular slotted defected ground structure (QSDGS) that incorporates a wide band microstrip antenna (WMA) was proposed for 5G n46/n47/n79 and n102 band applications. The DGS was represented on the ground plane by four rectangular looped slots. An inset feeding technique was employed on this slotted patch antenna. This DGS loaded patch antenna structure was mounted on an RT Duriod 5880 (ε_r = 2.2, loss tangent = 0.0009) with dimensions of $33 \times 29 \times 1.5\,\text{mm}^3$ ($0.44\lambda \times 0.38\lambda \times 0.02\lambda$, where '$\lambda$' is calculated at the lowest operating wavelength). This embedded antenna radiating structure resonated in a wide band ranging from 4.03 GHz to 6.32 GHz giving an impedance bandwidth of 2.3 GHz (50%), with a centre frequency of 4.44 GHz. The maximum gain was 4.7 dBi, and greater than 75% efficiency was obtained over the wide band. From the results extracted from the proposed antenna, it was found that the antenna was capable of covering the 5G NR n46/n47/n79 and n102 bands with significant bandwidth, gain, and efficiency. Thus, the antenna can be considered a potential contender for 5G mid-band wireless communication systems.

1. INTRODUCTION

The ever-increasing volume of data sent and the number of connected devices have far-reaching consequences on people's personal and professional lives. It was foreseen that by 2020, the number of mobile networking devices would surpasse 100 billion, thanks to the rapid rise of wireless cellular infrastructure and the ongoing expansion of the Internet of Things [1]. Because the number of user devices is growing at such a fast rate, there is a greater need for bandwidth in order to handle the ever-increasing volume of data [2]. The most distinctive characteristics of 5G technologies are the relatively fast transmission of data, the avoidance of any delay, and the wider availability of connectivity. For highly populated urban regions where connection demand is strong, the 5G mid-band offers a compromise of penetration, coverage, speed, and capacity [3]. The development of antennas for contemporary mobile devices is a difficult endeavor, according to all reports. The development of future global standards for 5G networks needs antennas that are much more compact while retaining their capabilities. The design of an antenna is ascertained by the operating frequency as well as the needed bandwidth [4–6].

The implementation of sub-6 GHz and mm-wave frequencies presents additional hurdles for fifth generation wireless antennas because the main determinants including high bandwidth and decreased multipath fading, design flexibility, quality, and performance are full of concerns. In [7], an 8-element dual-band MIMO antenna is proposed with a $150 \times 75\,\text{mm}^2$ dimension and is intended for the use

Received 9 February 2023, Accepted 22 May 2023, Scheduled 28 May 2023

* Corresponding author: Idrish Shaik (idrishshaik@gmail.com).

[1] ECE Department, Andhra University, Vishakapatnam, India. [2] ECE Department, GVP College for Degree and PG Courses (Autonomous), Vishakapatnam, India.

with 3.1–3.78 GHz and 5.4–6.21 sub-6 GHz networks. Over 12 dB of separation was measured between elements. However, it only achieved a gain of 2.5 dBi and 5 dBi across narrow bandwidths of 680 MHz and 780 MHz on its dual bands. In [8], a novel monopole coplanar waveguide (CPW) antenna incorporating artificial magnetic conductor (AMC) structures operate from 2.37 GHz to 2.5 GHz and from 4.45 GHz to 4.9 GHz, which achieves gains of 5 dBi and 7 dBi but extremely narrow bandwidths with greater dimensions of $79.9 \times 79.9 \times 8\,\text{mm}^3$. A $28 \times 26.35 \times 1.6\,\text{mm}^3$ reconfigurable monopole antenna with dip switch was presented in [9] which had a gain of only 1.38–4.89 dBi but an efficiency of 97.66%.

The 3.20–5.34 GHz working band of a miniaturised wideband antenna was suggested in [10] for the use in sub-6 GHz applications. The maximal gain for this radiator is only 2.4 dBi, despite its high 96% efficiency. A $30 \times 20 \times 1.5\,\text{mm}^3$ wideband 3.15–5.55 GHz multi-slotted antenna was proposed in [11]. This planar antenna has a 2.69 dBi gain and 79.6% efficiency. In [12], a dual-band elliptical ring patch fabricated on a low-cost FR4 substrate was presented for 5G wireless networks. This patch antenna achieved a gain of 6.1 dBi in the operational range of 3.28–3.78 GHz; nevertheless, its unusually large dimensions of $180 \times 60 \times 1.6\,\text{mm}^3$ resulted in a bandwidth of just 500 MHz. For a band of 4.6–6.1 GHz, the massive gain of 11.4–15.8 dBi was achieved using a circularly polarised antenna in [13] equipped with parasitic elements, despite its enormous dimensions of $110 \times 110 \times 3.4\,\text{mm}^3$. Using a size of $150 \times 75\,\text{mm}^2$, a 4-element MIMO antenna of 3.21–3.81 GHz was presented in [14]. Even though the maximal gain was just 3.69 dBi, it was able to provide the isolation of > 10 dB at 90% efficiency. In [15], a two-element triangular patch microstrip antenna array with a defective hexagonal ground structure was constructed for operation at 2.65 GHz. Exceptionally large in size at $105 \times 130\,\text{mm}^2$, this antenna had a gain above 11 dBi. DGS has been utilized in the field of microstrip antennas in order to improve the radiation characteristics of the microstrip antenna by increasing the bandwidth and gain of the microstrip antenna, as well as suppressing higher mode harmonics and cross-polarization [16].

To overcome those challenges and meet the requirements of the 5G sub-6 GHz spectrum, this proposed novel design offers a low complexity, small-scale, wide spectrum range with dimensions of $33 \times 29 \times 1.5\,\text{mm}^3$ and electrical dimensions of $0.44\lambda \times 0.38\lambda \times 0.02\lambda$ for 5G mid-band applications. It resonates at 4.4 GHz and has an impedance bandwidth of 2.3 GHz (4–6.32 GHz) with a peak gain of 4.75 dB, making it suitable for broadband. The antenna presented in this paper is composed of a patch with multiple vertical slots mounted on a Rogers 5880 substrate and a quadrangular slotted defected ground plane at the bottom. The structure of the paper is as follows. The design process for the antenna is covered in Section 2. The performance of the antenna is shown in relation to its physical features, and the experiment's findings are presented in Section 3. Concluding evaluations are offered in the final section.

2. GEOMETRY OF ANTENNA DESIGN

Figure 1 illustrates the antenna that has been proposed from both the top and bottom views. The numerically calculated antenna dimensions are $33 \times 29 \times 1.5\,\text{mm}^3$. The presented monopole is designed with RT Duriod 5880 as a substrate, which has a dielectric constant of 2.2, a loss tangent of 0.0009, and a thickness of 1.5 mm. With CST Studio Suite 2019, the structure, simulation, and evaluation of the structure are carried out. The ground is loaded with four quadrangular spirals slotted into multiple vertical slits in a patch. The excitation for the antenna is provided via a microstrip inset feed of 50 Ω. This combination enables the antenna to cover a wide bandwidth, which ranges from 4.03 to 6.32 GHz. The following predefined design equations are used for calculating the antenna parameters [6].

Equation (1) [6] that follows can be applied in order to determine the width W_p of the patch

$$W_p = \frac{c}{2f_o}\sqrt{\frac{2}{\varepsilon_r + 1}} \tag{1}$$

$$W_p = \frac{30}{2 * 4.4}\sqrt{\frac{2}{2.2 + 1}} = 2.686\,\text{cm (or) } 26.86\,\text{mm}$$

Equation (2) that is used to determine the effective dielectric constant of the patch is [6]

$$\varepsilon_{reff} = \frac{\varepsilon_r + 1}{2} + \frac{\varepsilon_r - 1}{2}\left[1 + 12\frac{h}{W_p}\right]^{-\frac{1}{2}} \tag{2}$$

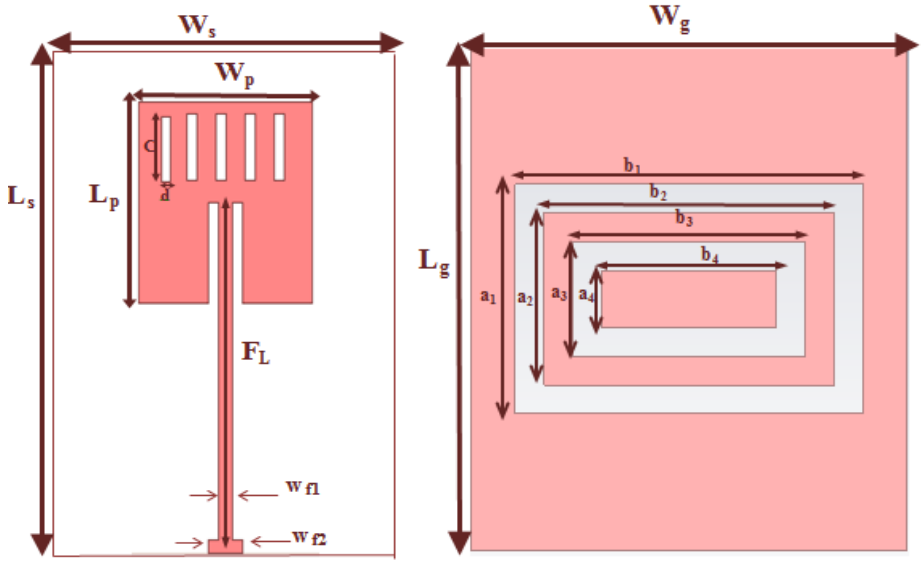

Figure 1. Posited antenna geometry. (a) Multiple slits patch structure. (b) Quadrangular spiral slotted ground structure.

$$\varepsilon_{eff} = \frac{2.2+1}{2} + \frac{2.2-1}{2}\left[1 + 12\frac{0.15}{2.686}\right]^{-\frac{1}{2}} = 2.056$$

The extended incremental length of the patch can be calculated using the following Equation (3) [6]

$$\Delta L = 0.412h\frac{(\varepsilon_{reff}+0.3)\left(\frac{W_p}{h}+0.264\right)}{(\varepsilon_{reff}-0.258)\left(\frac{W_p}{h}+0.8\right)} \tag{3}$$

$$\Delta L = 0.412\,h\frac{(2.056+0.3)\left(\frac{2.686}{0.15}+0.264\right)}{(2.056-0.258)\left(\frac{2.686}{0.15}+0.8\right)} = 0.0825\,\text{cm (or) } 0.82\,\text{mm}$$

Through the use of Equation (4), the effective length of the patch may be determined [6]

$$L_{eff} = \frac{c}{2f\sqrt{\varepsilon}_{reff}} \tag{4}$$

$$L_{eff} = \frac{c}{2*4.4\sqrt{2.056}} = 2.384\,\text{cm (or) } 23.84\,\text{mm} \tag{5}$$

By using Equation (5), the actual length of the patch, L_p, can be calculated [6]

$$L_p = L_{eff} - 2\Delta L \tag{6}$$

$$L_p = 2.384 - 2*0.082 = 2.22\,\text{cm (or) } 22.2\,\text{mm}$$

The typical patch of the antenna that should resonate at 4.4 GHz should have dimensions of $27\times22\,\text{mm}^2$, according to the calculations given in the aforementioned Equations (1)–(5). Through the use of miniaturization, the suggested multiple-slit patch was designed with dimensions of just $10\times10\,\text{mm}^2$, and the overall dimensions of the proposed antenna are $33\times29\times1.5\,\text{mm}^3$.

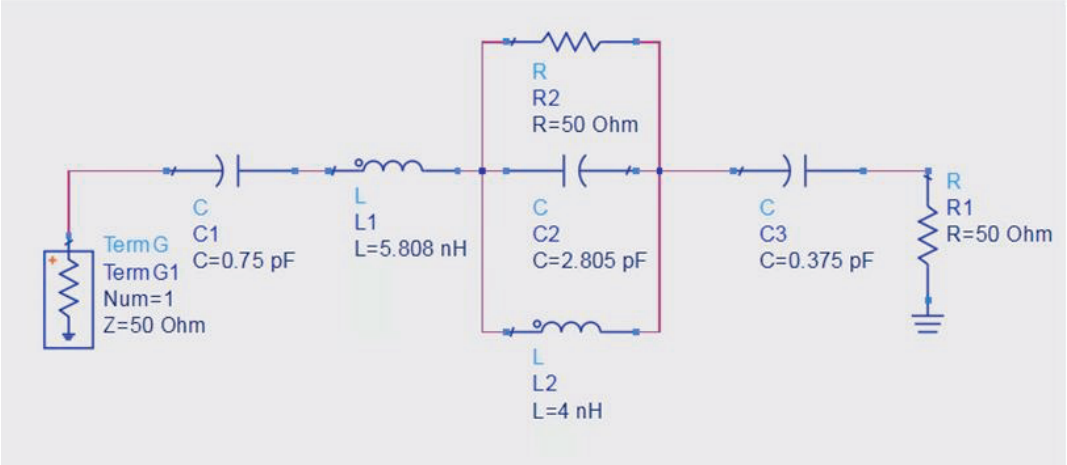

Figure 2. Equivalent circuit of the proposed antenna.

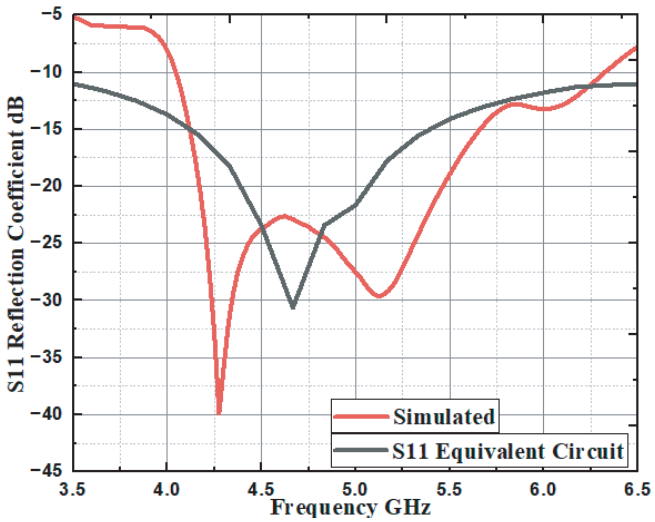

Figure 3. S_{11} return loss plot of equivalent circuit and simulated antenna.

Figure 2 depicts the equivalent circuit for the suggested design using RLC components. The circuit is designed with the aid of Advanced Design System (ADS) software. Low capacitance values have been chosen in the equivalent circuit in Figure 2, as a result of which precise s-parameters have been obtained, corresponding to those from the simulated design.

The return loss plots of the equivalent circuit and the proposed simulated S_{11} are shown in Figure 3. The impedance bandwidth is around 1 GHz, which is significantly smaller than the simulated impedance bandwidth, and the S_{11} reflection coefficient of the equivalent circuits is -29 dB at 4.6 GHz. From the observation, it is evident that the proposed antenna's power consumption is extremely low and has good significant characteristics.

2.1. Proposed Antenna Design Evolution Process

Figure 4 provides an illustration of each of the three stages that combine the evaluation process of the posited antenna. Figure 5 provides the S_{11} plot of the antenna evolution process of three stages. The patch and ground are designed using the dimensions specified in Table 1. In Stage 1 of the process a single tetragonal slot inserted into the ground reveals that most of the electric field is centered. This

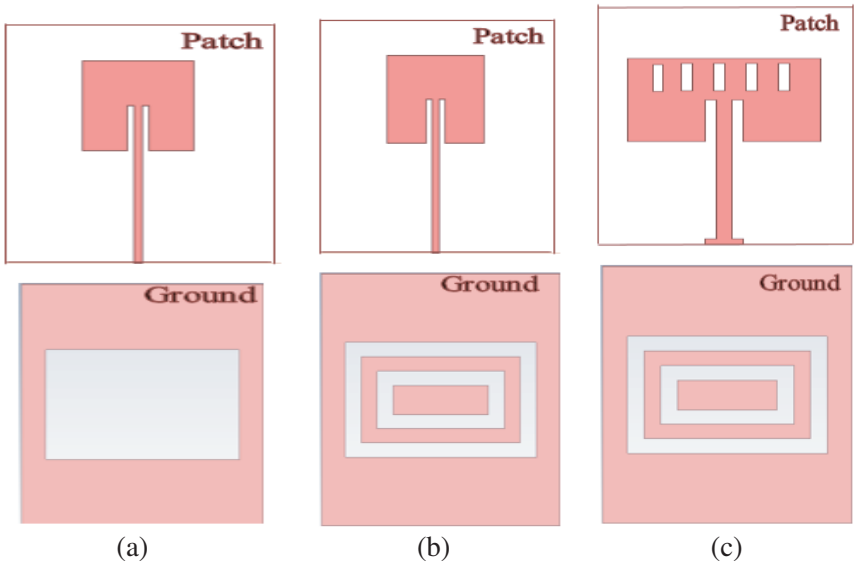

Figure 4. Antenna design evolution procedure. (a) Stage 1. (b) Stage 2. (c) Stage 3.

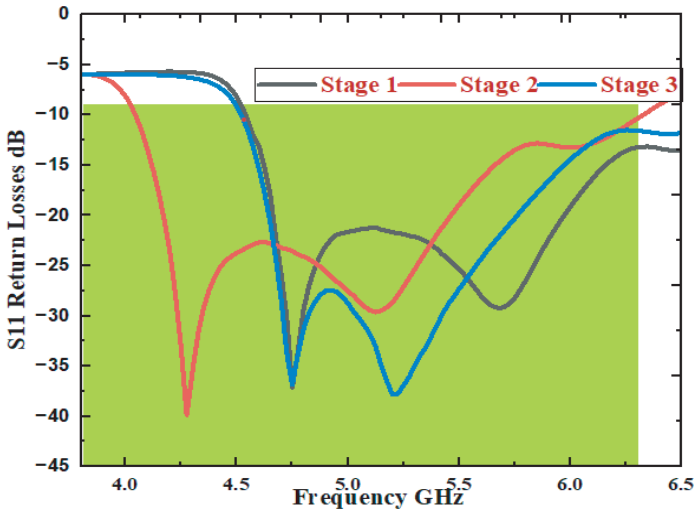

Figure 5. S_{11} return loss plot of various stages of antenna design evolution process.

Table 1. Calculated numerical design parameters of proposed antenna design in mm.

Parameter	$\mathbf{L_p}$	$\mathbf{W_p}$	$\mathbf{F_L}$	$\mathbf{W_{f1}}$	$\mathbf{W_{f2}}$	**Ls & Lg**	**Ws & Wg**	**C**	**d**
Dimensions	10	10	17.5	1	2	33	29	1	0.2
Parameter	$\mathbf{a_1}$	$\mathbf{a_2}$	$\mathbf{a_3}$	$\mathbf{a_4}$	$\mathbf{b_1}$	$\mathbf{b_2}$	$\mathbf{b_3}$	$\mathbf{b_4}$	**h**
Dimensions	16	12	8	4	24	20	16	12	1.5

gives a bandwidth of approximately 1.9 GHz. In stage 2, the ground plane has been modified to include three rectangular slots. In order to lessen the amount of cross-polarized radiation that is emitted by a monopole radiator, a four quadrangular slot defective ground structure has been suggested as a solution. These slots concentrate more electric field in the loop slots, allowing for a wider bandwidth of 2.3 GHz. Because of the loop slots in the ground structure, the bandwidth was increased, and in order to get

the patch element to resonate at the desired frequency, multiple vertical slits were placed on the patch element in stage 3 which can be seen in Figure 5. This was the main objective of having multiple slits. It was also observed that the addition of several vertical slits resulted in a considerable improvement in return loss at the resonating frequency, and it was increased to −37 dB which can be seen in Figure 5.

3. RESULTS WITH DISCUSSION

In this part, a detailed review of measured findings and simulated results is presented, along with an analysis of the proposed antenna performance based on a variety of different performance measures.

3.1. Reflection Coefficient

Figure 6 shows a plot of the computed and measured impedance spectrum values for the intended antenna. The antenna design that was proposed has a bandwidth of 2.3 GHz (50%), which allows it to cover a frequency band that ranges from 4.03 to 6.32 GHz. The results from simulation and experiment have been proven in good agreement and are acceptable for the usage in applications requiring 5G connectivity.

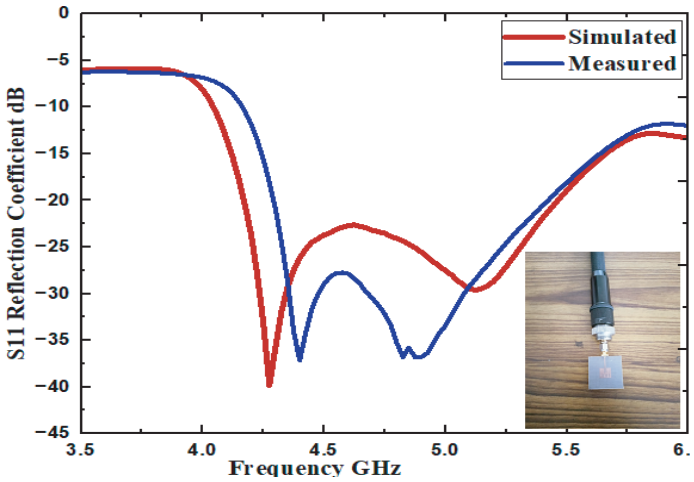

Figure 6. Computed and experimented return loss S_{11} of proposed antenna.

3.2. Surface Current Distribution

The current excitation of the simulated antenna is shown and illustrated in Figure 7 which shows the antenna in operation at its resonant frequency of 4.4 GHz. Figures 7(a) and 7(b) clearly show that the current distribution could be seen at the inset feed and defective ground structure.

3.3. Radiation Efficiency and Gain

Figure 8 provides an illustration of the proposed antenna's efficiency and gain. Figure 8(a) gives the minimum as well as maximum radiation efficiencies, which range from 65 to 81%, and Figure 8(b) clearly shows the maximum gain of 4.71 dB at 6.3 GHz and 4.2 dB at resonating frequency of 4.4 GHz, and the overall gain obtained in the frequency range is more than 4.1 dB.

3.4. Characteristics of Electromagnetic Radiation

The Three-dimensional gain plots of projected antenna structure are shown in Figures 9(a), (b), and (c) for the resonant frequencies of 4.2 GHz, 4.4 GHz, and 6.3 GHz. It is observed that from Figure 9(a) the gain of 4.11 dB was achieved, and 4.51 dB of gain was obtained at resonating frequency of 4.4 GHz shown in Figure 9(b). Figure 9(c) shows the 3D gain plot at 6.3 GHz, and 4.79 dB was obtained.

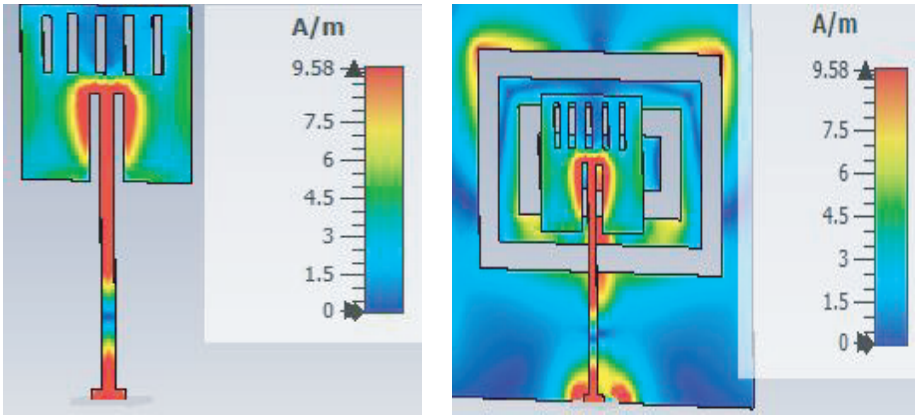

(a) (b)

Figure 7. (a) Current excitation of posited antenna in patch at 4.4 GHz. (b) Current excitation of posited antenna in patch and ground at 4.4 GHz.

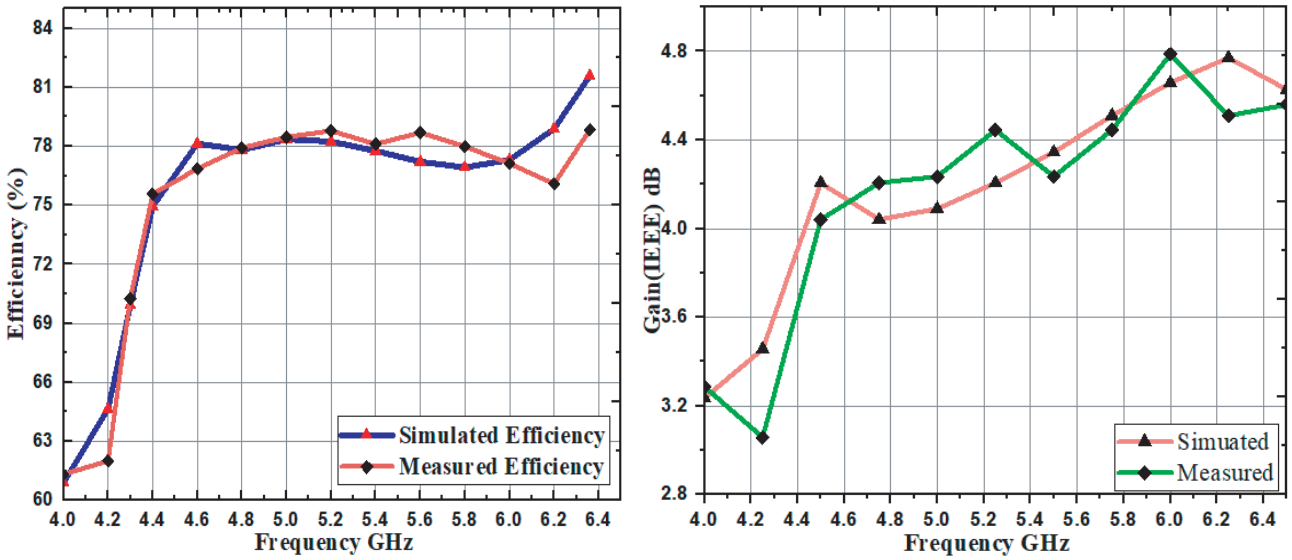

(a) (b)

Figure 8. (a) Measured and simulated efficiency plot at 4.4 GHz. (b) Measured and simulated gain plot at 4.4 GHz.

The far field pattern of radiation from the developed antenna design for the resonant frequency of 4.4 GHz is shown in Figure 10. The computed and measured radiation patterns of two major planes E-plane (XZ, $\emptyset = 0°$) and H-plane (YZ, $\emptyset = 90°$) are omnidirectional and bidirectional and can be seen in Figure 10.

The suggested antenna is modelled using CST 2019 software, and a Rogers 5880 is used to fabricate a prototype of the antenna for the usage in practical applications.

The top and bottom views of the fabricated element are shown in Figures 11(a) and 11(b). The proposed antenna was tested in an anechoic chamber using VNA N5247A.09.90.02 which can be seen in Figures 12(a) and 12(b).

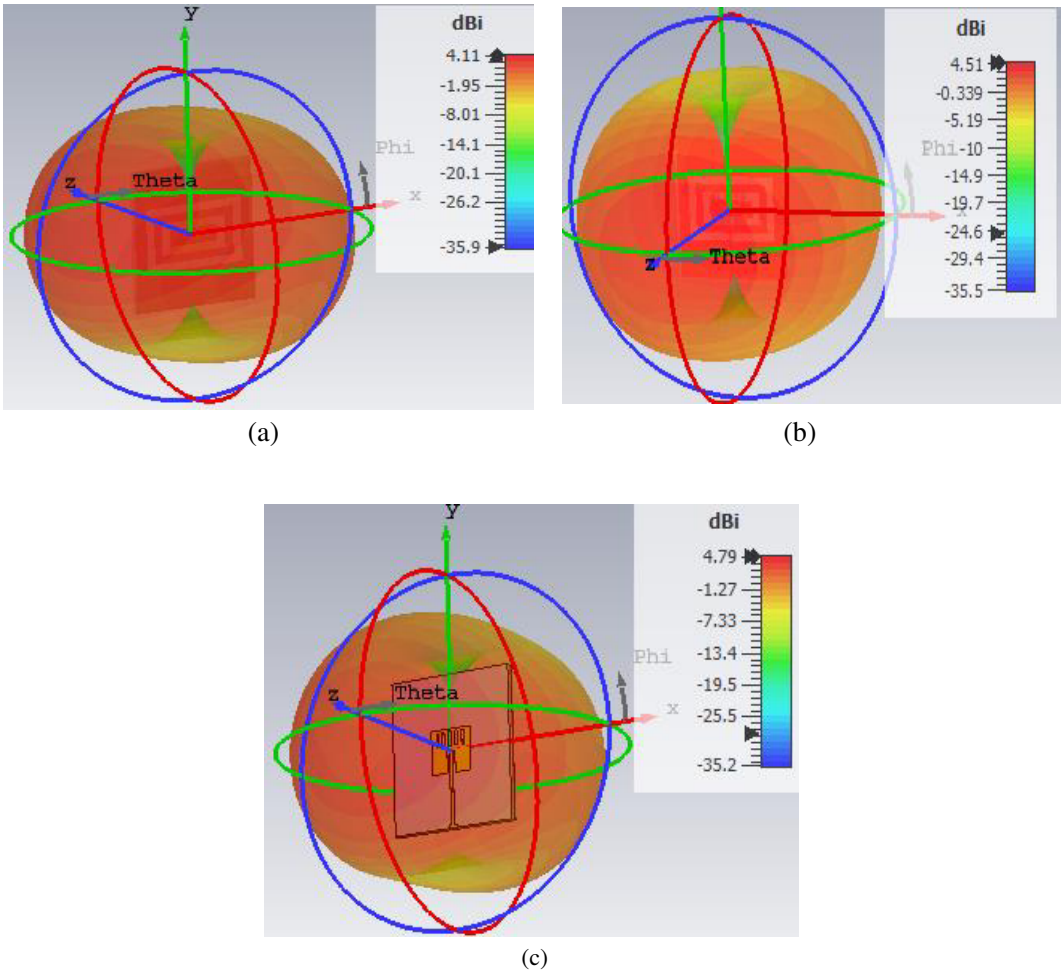

Figure 9. (a) 3D gain plot at 4.1 GHz. (b) 3D gain plot at 4.4 GHz. (c) 3D plot at 6.3 GHz.

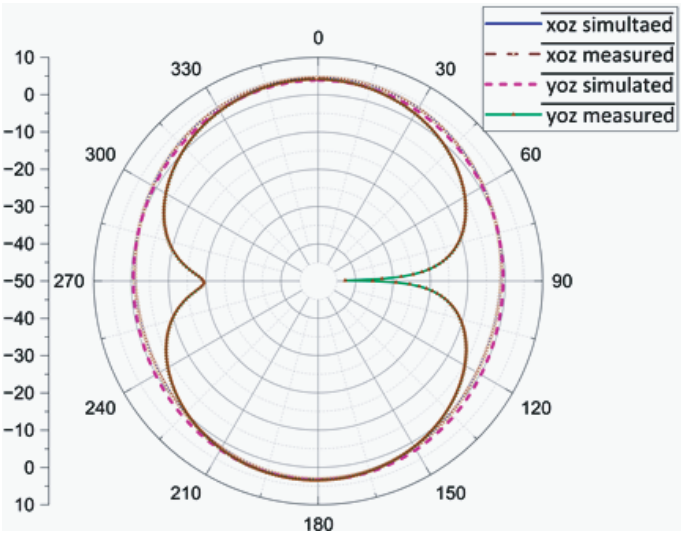

Figure 10. Simulated and measured far field radiation patterns of E and H plane at 4.4 GHz.

3.5. Comparative Analysis

Table 2 compares the designed antenna to studies published in previous works. The proposed antenna possesses beneficial radiation characteristics, including a wider bandwidth, steady gain, and high radiation efficiency. These characteristics give support to the concept that the design is acceptable with connection to systems of communication that operate within the sub-6 GHz band.

Table 2. Comparison of the designed antenna results with previous works.

Reference	Tuned Frequency (GHz)	Dimensions (mm^2)	No. of Elements	Bandwidth (GHz)	Gain (dB)	Radiation Efficiency (%)
[17] (2021)	3.72–3.82, 4.65–4.76 & 6.16–6.46	32×32	4	0.1, 0.1 & 0.3	2.5	89
[18] (2022)	2.67-4.20	40×40	1	1.53	3.92	95
[19] (2021)	2.44–2.54 & 3.19–3.55	46×46	1	0.1 & 0.36	4	-
[20] (2020)	3.3-4.0	40×30	1	0.7	2.5	-
[21] (2020)	3.89–5.9	78×58	-	2.01	3	80
[22] (2019)	2.75–5.45	130×130	1	2.7	8.4	80
[23] (2021)	1.82–2.92, 3.15–4.75	45×45	1	0.1, 1.6	4.8 & 7.5	-
[24] (2017)	1.95–2.5 3.15-3.85 4.95-6.6	100×150	4	0.55, 0.7 & 1.65	2.5, 3.7 & 4.4	-
[25] (2021)	1.85–3.8	48×35	1	1.95	4.04	92
[26] (2021)	2.8–3.81	36×36	1	1.01	4.08	-
[27] (2018)	3.1–3.75	34×34	1	0.65	3.	-
[28] (2019)	2.37 to 2.67 3.39 to 3.62	100×100	1	0.3 & 0.2	6	69.5
[29] (2019)	2.3–3.7	49.5×49.5	1	1.4	4	-
Proposed	4.03–6.32	33×29	1	2.3	4.1–4.75	65–81

- Not Mentioned

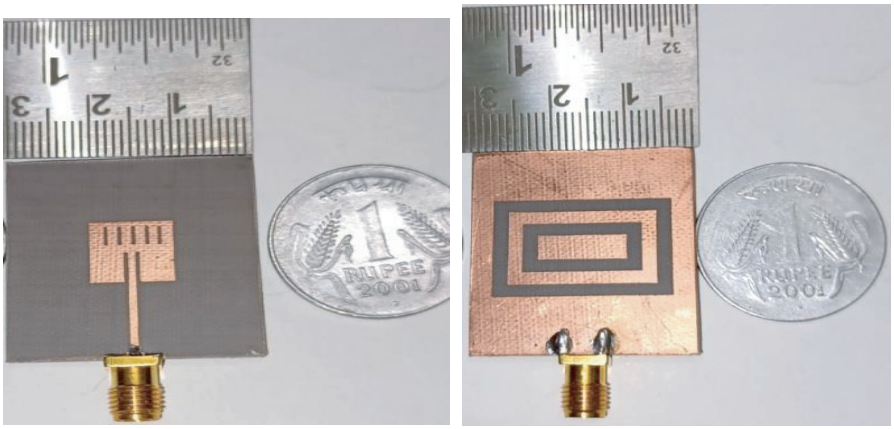

(a) (b)

Figure 11. (a) Top layer of the designed and manufactured antenna. (b) Bottom layer of the design and manufactured antenna.

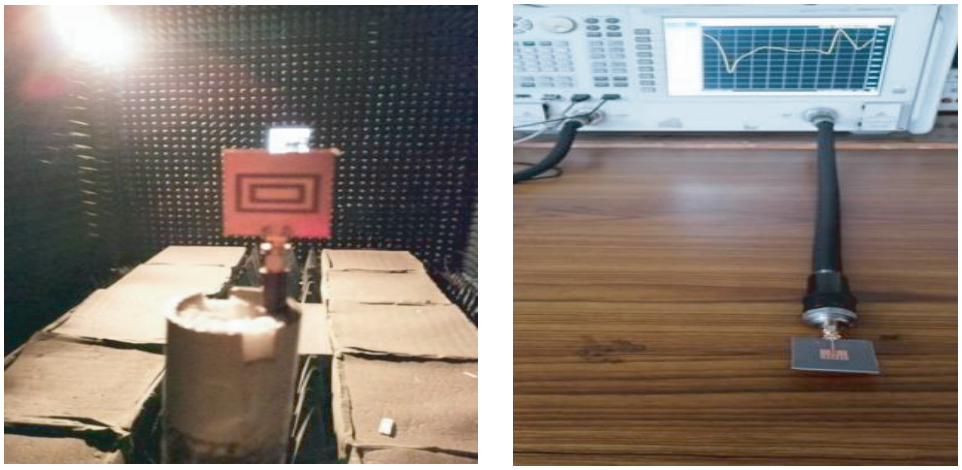

(a) (b)

Figure 12. (a) Antenna under test in anechoic chamber. (b) Proposed antenna under test using VNA N5247A.09.90.02.

4. CONCLUSION

A small-scale, high performance novel quadrangular slotted DGS with monopole antenna has been thoroughly presented to report a wide bandwidth of 2.3 GHz (50%) ranging from 4.02 to 6.32 GHz. The design includes multiple slots in a patch and a spiral-slotted DGS to offer high bandwidth and the required resonating frequency. The design was implemented on a Rogers's 5880 substrate, which has a frequency centre of 4.4 GHz, and it works significantly better than the antennas described in the previous works. Based on results of both measured and simulated data, a significant reflection coefficient of −37 dB is obtained by the proposed antenna at 4.4 GHz which has a bandwidth of 2.3 GHz, a gain of 4.1–4.7 dBi over the operating band, and a peak gain of 4.75 dBi at 6.3 GHz. The analysis of the proposed antenna in the previous work shows that the designed antenna is feasible for 5G sub-6 GHz mid-band applications like ultra-high definition multimedia, which require high data rates and bandwidth, especially in cellular infrastructure.

ACKNOWLEDGMENT

The authors would like to use this opportunity to acknowledge their gratitude to the administrations of both Bapatla Engineering College and GVPCDPGC for their support with this endeavor.

REFERENCES

1. Attaran, M., "The impact of 5G on the evolution of intelligent automation and industry digitization," *Journal of Ambient Intelligence and Humanized Computing*, 2021.
2. Cao, Y., K.-S. Chin, W. Che, W. Yang, and E. S. Li, "A compact 38 GHz multibeam antenna array with multifolded Butler matrix for 5G applications," *IEEE Antennas and Wireless Propagation Letters*, Vol. 16, 2996–2999, 2017.
3. Al-Gburi, A. J., Z. Zakaria, H. Alsariera, et al., "Broadband circular polarised printed antennas for indoor wireless communication systems: A comprehensive review," *Micromachines*, Vol. 13, No. 7, 1048, 2022.
4. Ikram, M., E. A. Abbas, N. Nguyen-Trong, K. H. Sayidmarie, and A. Abbosh, "Integrated frequency-reconfigurable slot antenna and connected slot antenna array for 4G and 5G mobile handsets," *IEEE Transactions on Antennas and Propagation*, Vol. 67, No. 12, 7225–7233, 2019.
5. Shafi, M., A. F. Molisch, P. J. Smith, et al., "5G: A tutorial overview of standards, trials, challenges, deployment, and practice," *IEEE Journal on Selected Areas in Communications*, Vol. 35, No. 6, 1201–1221, 2017.
6. Balanis, C. A., *Antenna Theory: Analysis and Design*, John Wiley and Sons, 2016.
7. Zahid, M. N., Z. Gaofeng, S. H. Kiani, et al., "H-shaped eight-element dual-band MIMO antenna for sub-6 GHz 5G smartphone applications," *IEEE Access*, Vol. 10, 85619–85629, 2022.
8. Abdelghany, M. A., M. Fathy Abo Sree, A. Desai, and A. A. Ibrahim, "Gain improvement of a dual-band CPW monopole antenna for sub-6 GHz 5G applications using AMC structures," *Electronics*, Vol. 11, No. 14, 2211, 2022.
9. Abd, A. K., J. M. Rasool, Z.-A. S. Rahman, and Y. I. Al-Yasir, "Design and analysis of novel reconfigurable monopole antenna using DIP switch and covering 5G-sub-6-GHz and C-band applications," *Electronics*, Vol. 11, No. 20, 3368, 2022.
10. Kapoor, A., R. Mishra, and P. Kumar, "Wideband miniaturized patch radiator for sub-6 GHz 5G devices," *Heliyon*, Vol. 7, No. 9, 2021.
11. Azim, R., A. K. M. M. H. Meaze, A. Affandi, et al., "A multi-slotted antenna for LTE/5G sub-6 GHz wireless communication applications," *International Journal of Microwave and Wireless Technologies*, Vol. 13, No. 5, 486–496, 2020.
12. Arya, A. K., S. J. Kim, and S. Kim, "A dual-band antenna for LTE-R and 5G lower frequency operations," *Progress In Electromagnetics Research Letters*, Vol. 88, 113–119, 2020.
13. Tran, H. H. and H. C. Park, "Gain and bandwidth enhancements of sequential-fed circularly polarized patch antenna array using multiple parasitic elements," *International Journal of RF and Microwave Computer-Aided Engineering*, Vol. 30, No. 9, 2020.
14. Rafique, U., S. Khan, M. M. Ahmed, et al., "Uni-planar MIMO antenna for sub-6 GHz 5G mobile phone applications," *Applied Sciences*, Vol. 12, No. 8, 3746, 2022.
15. Zulkifli, F. Y., E. T. Rahardjo, and D. Hartanto, "Radiation properties enhancement of triangular patch microstrip antenna array using hexagonal defected ground structure," *Progress In Electromagnetics Research M*, Vol. 5, 101–109, 2008.
16. Khandelwal, M. K., B. K. Kanaujia, and S. Kumar, "Defected ground structure: Fundamentals, analysis, and applications in modern wireless trends," *International Journal of Antennas and Propagation*, Vol. 2017, 1–22, 2017.
17. Krishnamoorthy, R., A. Desai, R. Patel, and A. Grover, "4 element compact triple band MIMO antenna for sub-6 GHz 5G wireless applications," *Wireless Networks*, Vol. 27, No. 6, 3747–3759, 2021.

18. Paul, L. C., H. K. Saha, T. Rani, et al., "An omni-directional wideband patch antenna with parasitic elements for sub-6 GHz band applications," *International Journal of Antennas and Propagation*, Vol. 2022, 1–11, 2022.
19. Nelaturi, S., "ENGTL based antenna for Wi-Fi and 5G," *Analog Integrated Circuits and Signal Processing*, Vol. 107, No. 1, 165–170, 2021.
20. Kapoor, A., R. Mishra, and P. Kumar, "Compact wideband-printed antenna for sub-6 GHz fifth-generation applications," *International Journal on Smart Sensing and Intelligent Systems*, Vol. 13, No. 1, 1–10, 2020.
21. Desai, A., T. Upadhyaya, J. Patel, R. Patel, and M. Palandoken, "Flexible CPW fed transparent antenna for WLAN and sub-6 GHz 5G applications," *Microwave and Optical Technology Letters*, Vol. 62, No. 5, 2090–2103, 2020.
22. Huang, B., W. Lin, J. Huang, et al., "A patch/dipole hybrid-mode antenna for sub-6 GHz communication," *Sensors*, Vol. 19, No. 6, 1358, 2019.
23. Yu, Z., L. Huang, Q. Gao, and B. He, "A compact dual-band wideband circularly polarized microstrip antenna for sub-6G application," *Progress In Electromagnetics Research Letters*, Vol. 100, 99–107, 2021.
24. Ramachandran, A., S. Mathew, V. Rajan, and V. Kesavath, "A compact triband quad-element MIMO antenna using SRR ring for high isolation," *IEEE Antennas and Wireless Propagation Letters*, Vol. 16, 1409–1412, 2017.
25. Singh, H., N. Mittal, A. Gupta, et al., "Metamaterial integrated folded dipole antenna with low SAR for 4G, 5G and Nb-IOT applications," *Electronics*, Vol. 10, No. 21, 2612, 2021.
26. Swetha, R. and A. Lokam, "Novel design and characterization of wide band hook shaped aperture coupled circularly polarized antenna for 5G application," *Progress In Electromagnetics Research C*, Vol. 113, 161–175, 2021.
27. Al-Yasir, Y., A. Abdullah, N. Ojaroudi Parchin, R. Abd-Alhameed, and J. Noras, "A new polarization-reconfigurable antenna for 5G applications," *Electronics*, Vol. 7, No. 11, 293, 2018.
28. Jin, G., C. Deng, J. Yang, Y. Xu, and S. Liao, "A new differentially-fed frequency reconfigurable antenna for WLAN and sub-6 GHz 5G applications," *IEEE Access*, Vol. 7, 56539–56546, 2019.
29. Zhao, L., Z.-M. Chen, and J. Wang, "A wideband dual-polarized omnidirectional antenna for 5G/WLAN," *IEEE Access*, Vol. 7, 14266–14272, 2019.